Bulk nanocomposite magnets produced by dynamic shock compaction

K. H. Chen and Z. Q. Jin
School of Materials Science and Engineering, Georgia Institute of Technology, Atlanta, Georgia 30332 and Department of Physics, University of Texas at Arlington, Arlington, Texas 76019

J. Li, G. Kennedy, Z. L. Wang, and N. N. Thadhani
School of Materials Science and Engineering, Georgia Institute of Technology, Atlanta, Georgia 30332

H. Zeng
IBM T.J. Watson Research Center, Yorktown Heights, New York 10598 and Department of Physics, University of Texas at Arlington, Arlington, Texas 76019

S.-F. Cheng
Naval Research Laboratory, Washington, DC 20375

J. P. Liu[a)]
Department of Physics, University of Texas at Arlington, Arlington, Texas 76019

(Received 16 September 2003; accepted 21 April 2004)

Exchange-coupled $R_2Fe_{14}B/\alpha$-Fe (R=Nd or Pr) nanocomposite bulk magnets with nearly full density have been successfully produced by shock compaction of melt-spun powders. X-ray diffraction and transmission electronic microscopy analyses of the shock-consolidated compacts showed no grain growth upon compaction, in fact, a decrease in the crystallite size of both the hard and soft phases was observed. As a consequence, magnetic properties were retained and even improved after compaction. Hysteresis loops of the shock-consolidated powder compacts showed a smooth single-phaselike behavior, indicating effective exchange coupling between hard and soft magnetic phases. © *2004 American Institute of Physics.* [DOI: 10.1063/1.1760834]

The figure of merit for a permanent magnet is the energy product, which is a combination of magnetization and coercivity. Unfortunately, nature tends to give only one or the other: soft magnetic materials such as Fe and FeCo alloy have high magnetization while hard magnetic materials such as SmCo alloys have high coercivity but relatively low magnetization. Exchange-coupled hard/soft nanocomposite magnets combine the advantages of both hard and soft phases, and thereby offer the potential of providing much higher-energy product (predicted to be higher than 100 MG Oe) compared to their single-phase anisotropic hard magnet counterparts (64 MG Oe for NdFeB magnets).[1] Many efforts have been made in recent years to produce nanocomposite powders, thin films, and rapidly quenched ribbons.[2,3] Formation of self-assembled FePt based hard/soft nanocomposites with remarkably enhanced energy product (around 20 MG Oe) has also been reported recently.[4] However, fabrication of bulk exchange-coupled nanocomposite magnets still remains a great challenge.

Shock compaction employs a variety of gas-gun and explosive loading devices that provide the rapid deposition of energy into the powders by shock waves of microseconds time duration thereby retaining the starting metastable or nanoscale structure.[5,6] Shock compaction has been reported for processing bulk microcrystalline and nanocrystalline single-phase magnetic alloys.[7–11] Here, we report on preparation and characterization of fully dense shock-compacted bulk nanocomposite magnets made from melt-spun $R_2Fe_{14}B/\alpha$-Fe (R=Nd or Pr) powders. The hard magnetic $Nd_2Fe_{14}B$ and $Pr_2Fe_{14}B$ alloys have very similar and practically indistinguishable structural, mechanical, and magnetic properties, and hence the two materials are simultaneously investigated in this work.

The starting samples used were obtained by pulverizing rapidly quenched and optimally annealed ribbons of $Nd_2Fe_{14}B$ and $Pr_2Fe_{14}B$ based nanocomposites with α-Fe content of 10 wt % and 20 wt %, respectively. The pulverized powders were cold pressed into steel capsules at 65%–78% of theoretical density. Shock-consolidation experiments were conducted using a three-capsule plate-impact fixture mounted at the end of an 80 mm diameter single-stage gas-gun barrel.[6] Impact of a projectile at velocities of 605, 880, and 950 m/s resulted in shock waves propagating through the capsules and compacting the powders, producing 12 mm diameter by 3 mm thickness discs. The interparticle bonding was observed using scanning electron microscopy (SEM). The crystallite size was characterized by x-ray diffraction (XRD) peak broadening analysis (Cu K_α radiation). Bright and dark field transmission electron microscopy (TEM) imaging was also performed to characterize the crystallite size. The magnetic properties were measured using a superconducting quantum interference device magnetometer with a maximum applied field of 70 kOe.

The dynamic and heterogeneous nature of plastic deformation during shock compaction of powders leads to localized deposition of shock energy at particle interfaces, which can produce subsequent melting and resolidification at inter-

a)Author to whom correspondence should be addressed; electronic mail: pliu@uta.edu

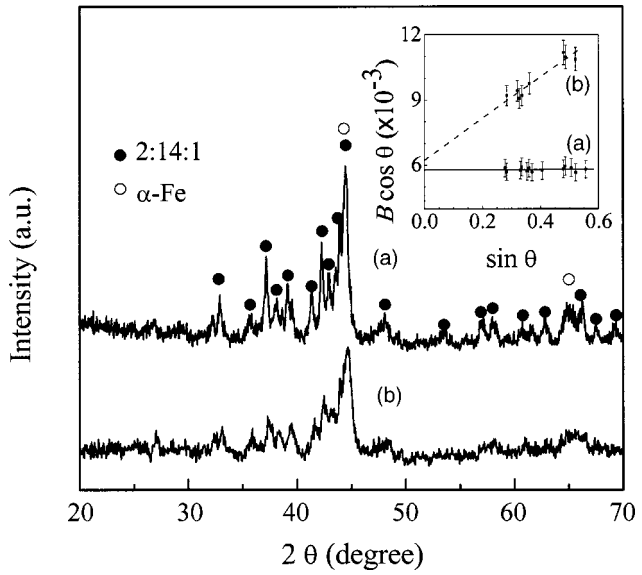

FIG. 1. SEM micrographs of fracture surface of NdFeB samples (a) shock consolidated at 950 m/s showing local melting, (b) shock consolidated at 605 m/s showing extensively deformation and laminar morphology. Both samples have density of 99%.

particle regions. The localized melting and resolidification were observed in the present study for the samples shock consolidated at 950 m/s, consistent with previous observations on explosively compacted single-phase Nd-Fe-B magnets.[9] Presence of such interparticle melted and resolidified regions can be detrimental to magnetic properties because of unfavorable grain growth or decomposition of magnetic phases. Optimization of the shock parameters, e.g., by adjusting initial packing density (via use of flake particles of 20–100 μm size) and lowering the impact velocity, allowed significant reduction and elimination of such defects in the present work. Powders pressed at initial packing density of 78% of theoretical density and impacted at velocity of 605 and 880 m/s resulted in nearly full density ($98.5\pm0.5\%$ of theoretical density) compacts of powders bonded in the solid state, with no evidence of local melting and resolidification at interparticle regions. The compact showed only features of plastic deformation and fracture of powder flakes. Because the starting powders are in the form of flakes, they have a tendency to align during initial uniaxial pressing, with the flat surfaces perpendicular to the pressing direction. It should be noted that the flakes in the compacted disk retain their alignment following shock compaction, which is a valuable attribute that can be exploited to obtain anisotropic magnets with highly oriented particles, for achieving further improvements in magnetic properties. The laminar morphology and solid state bonding were also observed in $Pr_2Fe_{14}B/\alpha$-Fe samples shock-consolidated at 880 m/s. The Vicker's microhardness of these $R_2Fe_{14}B/\alpha$-Fe ($R=$Nd or Pr) nanocomposites measured by Leco DM-400F microhardness tester were found to increase from 6 to 8 GPa for starting compacts to 9–12 GPa for compacts after consolidation, indicating a strong interparticle bonding in the nearly fully dense compacts.

Figure 1 shows XRD patterns comparing the structure of

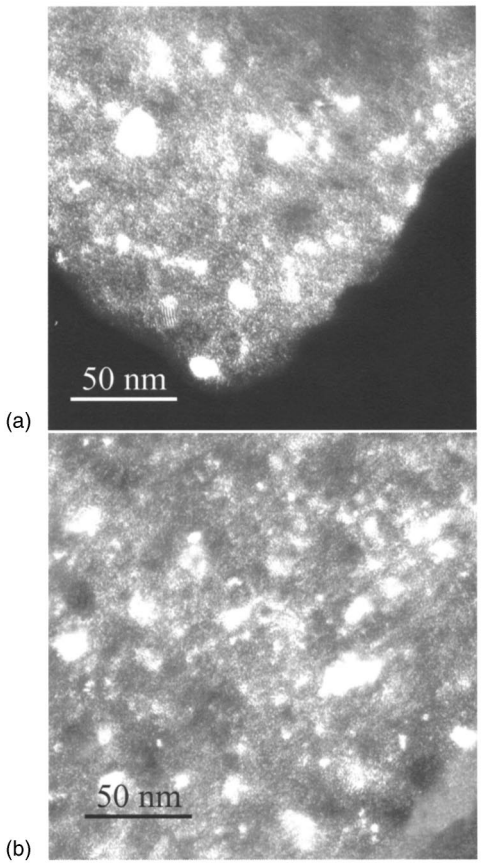

FIG. 2. TEM dark-field micrographs of grain morphology of (a) starting PrFeB materials and (b) center part of recovered shock-consolidated sample.

(a) starting $Pr_2Fe_{14}B/\alpha$-Fe material and (b) recovered compact shock consolidated at 880 m/s. The starting ribbon and the shock-consolidated compacts were ground prior to performing XRD analysis. XRD diffraction patterns of both samples match the peaks corresponding to those of hard magnetic $Pr_2Fe_{14}B$ and soft α-Fe phase. The shock-consolidated sample shows broadening of peaks for both the phases, with the peak broadening being more so for the α-Fe phase than for the hard phase. The broadening of the peaks may be related to microstrain and a decrease in the crystallite size caused by shock compression, both of which can be evaluated using the Williamson-Hall plots based on line-broadening analysis[12] as shown in inset of Fig. 1. The nearly zero slope indicates no microstrain in the starting ribbon powder, while the shock-consolidated sample shows extensive microstrain of $\sim 5.19\times10^{-3}$, typical of that observed in heavily cold-worked metallic materials. The larger intercept for the shock-consolidated sample reflects a possible decrease in the average grain size upon shock compaction. The corresponding values indicate an average grain size of 20 nm in shock-consolidated samples, compared to an average size of 25 nm in the starting powders.

The average grain size of the shock-consolidated compacts and its possible decrease from that of the starting powders were also confirmed by TEM analysis. Figures 2(a) and 2(b) respectively show representative dark field TEM images of the starting ribbon and the shock compacted $Pr_2Fe_{14}B/\alpha$-Fe nanocomposite samples. For the starting

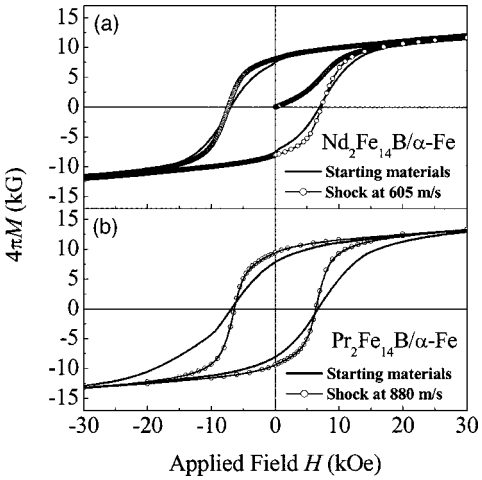

FIG. 3. Hysteresis loops of (a) starting $Nd_2Fe_{14}B/\alpha$-Fe nanocomposite powders and the recovered sample shock consolidated at 605 m/s, and (b) starting $Pr_2Fe_{14}B/\alpha$-Fe nanocomposite and the recovered sample shock consolidated at 880 m/s. No demagnetizing calibrations are made on the curves.

powder an average grain size of ~23 nm was measured, based on quantitative metallographic analysis performed on the dark-field image shown in Fig. 2(a). Dark-field imaging of the sample shock compacted at 880 m/s revealed retention of nanostructure. Furthermore, as shown in Fig. 2(b), many more fine bright-contrast dots representing crystallites are observed in the shock-consolidated sample. Quantitative analysis of grain size shows a bimodal distribution with one peak around 18 nm and another around 8 nm, indicating grain refinement caused by shock compaction of the powders. The refined grains observed in the shock-consolidated samples may be attributed to fragmentation and shearing of the nanocrystallites during dynamic compaction, which is similar to the results for shock-consolidated SmFeN reported in Ref. 8. The grain size retention and refinement are in fact important advantages of the shock-consolidation technique, and are essential for attaining optimal magnetic properties in nanocomposite magnets.

Figure 3 shows representative hysteresis loops for the starting $R_2Fe_{14}B/\alpha$-Fe (R=Nd or Pr) samples and the Nd-based sample shock consolidated at 605 m/s as well as the Pr-based sample shock consolidated at 880 m/s. The higher saturation magnetization in $Pr_2Fe_{14}B/\alpha$-Fe samples compared to the $Nd_2Fe_{14}B/\alpha$-Fe nanocomposites is attributed to its higher amount (20 wt %) of soft α-Fe phase. The corresponding energy products for the $Nd_2Fe_{14}B/\alpha$-Fe samples are calculated to be 8.3 MG Oe for the starting powders and 11.6 MG Oe, for shock-consolidated compacts (before demagnetization calibration). The shock-consolidated $Pr_2Fe_{14}B/\alpha$-Fe magnets showed a higher energy product of 13.9 MG Oe, while that of the corresponding starting powder was 8.6 MG Oe. After considering a demagnetization factor of 0.33 and 0.14 for starting Pr-Fe-B powder sample and the shock-compacted sample (estimated according to shapes of the specimens), respectively, the energy product values are estimated to be around 16.3 MG Oe for the shock compacted samples and 14.7 MG Oe for starting Pr-Fe-B material. It should be noted that these magnetic properties are superior to those of resin-bonded bulk magnets,[13] though still lower than that for aligned sintered magnets. Figure 3 also reveals that the hysteresis loops of the shock-consolidated samples have a smooth single-phaselike behavior and a high remanence ratio above the Stoner-Wolfarth value of $M_s/2$ expected for noninteracting isotropic single-domain particles. This result reveals that the magnetic properties of the staring nanocomposite powders have been well preserved and actually improved following shock compaction, which is directly related to the successful retention of the nanostructure (especially the nanoscale dimension of the soft phase) and the nearly full density of the compacts. The nanoscale grain size and intimate interparticle contacts lead to effective interphase exchange coupling in the shock-consolidated specimens.

In conclusion, shock compaction technique has been used to successfully produce fully dense of $R_2Fe_{14}B/\alpha$-Fe (R=Nd or Pr) bulk nanocomposite magnets. The nearly complete densification, retention, and refinement of nanostructure lead to improved magnetic properties. There is still considerable room for the improvement of magnetic properties through the improved quality of starting powders and possibly by use of pre-compaction or postcompaction heat treatments. It should be pointed out that while shock compaction using gas gun allows better correlation of properties and microstructure with controlled shock loading conditions, explosive shock-consolidation methods can also be used for production of bulk nanocomposite magnets of larger dimensions needed for practical applications. Our further work on the bulk $Pr_2Fe_{14}B/\alpha$-Fe nanocomposite magnets produced by explosive shock consolidation has also revealed retention of nanostructure and magnetic properties and will be presented elsewhere.

This work was supported by US DoD/DARPA through ARO under grant No. DAAD19-03-1-0038.

[1] R. Skomski and J. M. D. Coey, Phys. Rev. B **48**, 15812 (1993).
[2] Z. Q. Jin, H. Okumura, H. L. Wang, and G. C. Hadjipanayis, J. Appl. Phys. **91**, 8165 (2002).
[3] J. P. Liu, C. P. Luo, Y. Liu, and D. J. Sellmyer, Appl. Phys. Lett. **72**, 483 (1998).
[4] H. Zeng, J. Li, J. P. Liu, Z. L. Wang, and S. H. Sun, Nature (London) **420**, 395 (2002).
[5] W. H. Gourdin, Prog. Mater. Sci. **30**, 39 (1986).
[6] P. J. Counihan, A. Crawford, and N. N. Thadhani, Mater. Sci. Eng., A **267**, 26 (1999).
[7] R. Chau, M. B. Maple, and W. J. Nellis, J. Appl. Phys. **79**, 9236 (1996).
[8] M. Leonowicz, W. Kaszuwara, E. Jezierska, D. Januszewski, G. Mendoza, H. A. Davies, and J. Paszula, J. Appl. Phys. **83**, 6634 (1998).
[9] S. Ando, Y. Mine, K. Takashima, S. Itoh, and H. Tonda, J. Mater. Process. Technol. **85**, 142 (1999).
[10] S. I. Shkuratov, E. F. Talantsev, J. C. Dickens, M. Kristiansen, and J. Baird, Appl. Phys. Lett. **82**, 1248 (2003).
[11] M. W. Petrie and N. W. Page, Acta Metall. Mater. **40**, 3195 (1992).
[12] G. K. Williamson and W. H. Hall, Acta Metall. **1**, 22 (1953).
[13] H. Kanekiyo, M. Uehara, and S. Hirosawa, IEEE Trans. Magn. **29**, 2863 (1993).